Redox behaviour of the haem domain of flavocytochrome c_3 from *Shewanella frigidimarina* probed by NMR

Miguel Pessanha[a,1], Emma L. Rothery[b,1], Ricardo O. Louro[a], David L. Turner[c],
Caroline S. Miles[d], Graeme A. Reid[d], Stephen K. Chapman[b],
António V. Xavier[a], Carlos A. Salgueiro[a,e,*]

[a] *Instituto de Tecnologia Química e Biológica, Universidade Nova de Lisboa, Rua da Quinta Grande 6, 2780-156 Oeiras, Portugal*
[b] *Department of Chemistry, University of Edinburgh, West Mains Road, Edinburgh EH9 3JJ, UK*
[c] *School of Chemistry, University of Southampton, Southampton SO17 1BJ, UK*
[d] *Institute of Cell and Molecular Biology, University of Edinburgh, Mayfield Road, Edinburgh EH9 3JR, UK*
[e] *Departamento de Química da Faculdade de Ciências e Tecnologia da Universidade Nova de Lisboa, Quinta da Torre, 2825-114 Caparica, Portugal*

Abstract **Flavocytochrome c_3 from *Shewanella frigidimarina* (fcc₃) is a tetrahaem periplasmic protein of 64 kDa with fumarate reductase activity. This work reports the first example of NMR techniques applied to the assignment of the thermodynamic order of oxidation of the four individual haems for such large protein, expanding its applicability to a wide range of proteins. NMR data from partially and fully oxidised samples of fcc₃ and a mutated protein with an axial ligand of haem IV replaced by alanine were compared with calculated chemical shifts, allowing the structural assignment of the signals and the unequivocal determination of the order of oxidation of the haems. As oxidation progresses the fcc₃ haem domain is polarised, with haems I and II much more oxidised than haems III and IV, haem IV being the most reduced. Thus, during catalysis as an electron is taken by the flavin adenosine dinucleotide from haem IV, haem III is eager to re-reduce haem IV, allowing the transfer of two electrons to the active site.**

© 2004 Published by Elsevier B.V. on behalf of the Federation of European Biochemical Societies.

Keywords: Shewanella; Flavocytochrome; Fumarate respiration; Nuclear magnetic resonance; Electron transfer protein; Multihaem

1. Introduction

Flavocytochrome c_3 isolated from the bacterium *Shewanella frigidimarina* (fcc₃) is a 64-kDa monomeric and soluble periplasmic enzyme with unidirectional fumarate reductase activity [1]. This electron transfer protein is produced in large amounts by *Shewanella* spp. under anaerobic growth, and shows unique features when compared with other bacterial flavocytochromes that are multimeric, membrane bound and have bi-directionality activity [1,2]. The crystal structure of fcc₃ shows that it folds in three domains: the N-terminal haem domain containing four *c*-type haems with bis-histidinyl axial coordination; the flavin domain which contains a non-covalently bound flavin adenosine dinucleotide (FAD), located at the active site; and a mobile clamp domain (Fig. 1A) [3]. The spatial architecture of the five redox centres allows efficient conduction of electrons through the haem domain to the flavin active site, where fumarate is reduced to succinate (Fig. 1B) [3]. The electron transfer protein fcc₃ has been characterised structurally, thermodynamically and kinetically [1,3–12], but microscopic characterization of the individual haem redox centres has not been achieved. A macroscopic redox characterization of fcc₃, obtained by voltammetry studies, allowed the reduction potential of FAD to be determined [1], but not specifically those of each haem group. That study [1] also showed that only the FAD quinone and hydroquinone forms were observed on the time scale of the experiments, indicating that two electrons are accepted by FAD, in a cooperative fashion.

Detailed characterization of the mechanism of redox proteins containing several cofactors requires information on the redox condition of each centre in each of the various microscopic states of the protein. This is not easy when the centres are all of the same nature, making spectroscopic distinction difficult. The sensitivity of NMR to the environment of the nuclei gives this technique the required spectral discrimination. NMR has been used to determine the thermodynamic order in which each haem becomes oxidised at different oxidation stages throughout a redox titration (referred in the previous literature as order of oxidation of the haems [13–16]), as well as to probe in detail the network of redox and redox-Bohr (electron–proton) interactions of the centres of relatively small proteins, up to 16 kDa molecular weight, containing up to four haem groups or two [4Fe–4S] centres [13–28]. However, many proteins and enzymes of physiological interest do not fall in this favourable weight range for NMR studies. This work reports the first application of NMR techniques to the assignment of the order of oxidation of the individual haems of fcc₃ (64 kDa) and the concomitant elucidation of the haem redox behaviour of this large protein.

*Corresponding author. Fax: +351 21 4428766.
E-mail address:* cas@itqb.unl.pt (C.A. Salgueiro).

[1] These authors contributed equally to this work.

Abbreviations: fcc₃, *Shewanella frigidimarina* NCIMB400 flavocytochrome c_3; EXSY, exchange spectroscopy; FAD, flavin adenosine dinucleotide
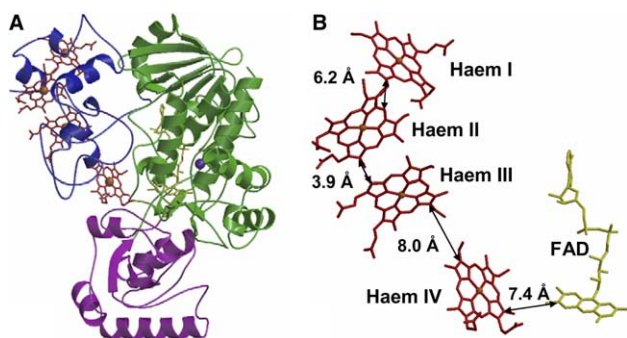
Fig. 1. Structural features of fcc$_3$ [3]. (A) Domain structure of fcc$_3$. The three domains of fcc$_3$ are coloured: haem domain (blue), flavin domain (green), and clamp domain (magenta). Haems are shown in red and FAD in yellow. (B) Spatial disposition of the five redox centres of the enzyme, labelled accordingly. The edge-to-edge distances between neighbouring centres are shown.

2. Materials and methods

2.1. Protein purification

The recombinant fcc$_3$ was purified as described in [4]. A mutated flavocytochrome c_3, in which the axial ligand of haem IV (His61) was replaced by the amino acid alanine (fcc$_3$H61A), was produced and purified as described in [11].

2.2. NMR sample preparation

For all NMR studies, the protein solutions were exchanged several times into 99.9% ^{2}H$_2$O using ultrafiltration methods (Amicon; YM-10). Samples with a final protein concentration of 0.5 mM were used. The ionic strength was adjusted to approx. 100 mM by addition of NaCl in ^{2}H$_2$O. Reduction of the samples was achieved by the reaction with gaseous hydrogen in the presence of catalytic amounts of the enzyme hydrogenase (isolated from *Desulfovibrio gigas* and *Desulfovibrio vulgaris*). Partially oxidised samples were obtained by first flushing out the hydrogen from the reduced sample with argon and then adding controlled amounts of air into the NMR tube with a syringe through the serum caps as previously described [27].

2.3. NMR spectroscopy

^{1}H NMR spectra were obtained in a 500-MHz Bruker DRX500 spectrometer equipped with a 5-mm inverse detection probe head with internal B_0 gradient coils and a Eurotherm 818 temperature control unit. For specific detection of high spin signals, ^{1}H NMR spectra were recorded in a 300-MHz Bruker AMX300 equipped with a 5-mm inverse detection probe head. Chemical shifts are reported in parts per million (ppm), relative to tetramethylsilane, and the proton spectra were calibrated using the water signal as internal reference.

2.3.1. NMR of oxidised fcc$_3$ and fcc$_3$H61A. One-dimensional (1D) spectra of fcc$_3$ and fcc$_3$H61A were acquired at 298 K at pH 7.0 and 8.5. The 1D spectra of fcc$_3$ and fcc$_3$H61A obtained at 500 MHz were acquired by collecting 64k data points to cover a sweep width of 32 kHz, with 128 scans. In order to evaluate the existence of low field high spin signals, additional 1D spectra of fcc$_3$ and fcc$_3$H61A were also collected at 300 MHz using a sweep width of 60 kHz.

2.3.2. NMR redox titrations of fcc$_3$ and fcc$_3$H61A. To establish the complete pattern of oxidation for each haem methyl group, several 2D-exchange spectroscopy (EXSY) NMR data sets were collected at 298 K and pH 7.0 and 8.5, in the 500-MHz spectrometer. These spectra were acquired with 25 ms mixing time using 4096 (t_2) × 1024 (t_1) data points spanning a sweep width of 32 kHz, with 128 scans per increment.

2.4. Predictions of chemical shifts for the haem methyls

The chemical shifts of the haem methyls were calculated at 298 K using the geometry of the haem axial ligands from the crystal structure. These were used as input for the empirical equation reported in the literature [29].

3. Results and discussion

The haem core architecture of the four haem groups in the N-terminal domain of fcc$_3$ is similar to that found in a small periplasmic tetrahaem cytochrome isolated from the same bacterium [15]. In the small tetrahaem cytochrome, all of the haem irons have bis-His axial coordination and they are low spin, both in the reduced and oxidised forms. Thus, the protein is diamagnetic when reduced (Fe(II), $S = 0$) and paramagnetic when oxidised (Fe(III), $S = 1/2$). This is convenient for NMR studies, since widely different well-resolved spectra are obtained for both oxidation states, making it easier to assign the order in which specific haems within the structure are oxidised. In fcc$_3$, the haem groups are always also low spin, but because of the large molecular weight and the associated slow tumbling rate of the protein, it was not possible to obtain sufficiently well-resolved spectra to assign the haem resonances unequivocally in both forms. However, after a careful optimization of the experimental conditions in partially oxidised fcc$_3$ samples (protein concentration, ionic strength, temperature, and pH), it was possible to reduce the line width of the NMR signals and observe cross-peaks connecting haem signals in different degrees of oxidation using 2D-EXSY NMR experiments (Fig. 2). The NMR spectra of partially oxidised fcc$_3$ samples at pH 8.5 showed that the protein exhibits fast intra-molecular ($>9.23 \times 10^4$ s^{-1}) and slow intermolecular ($<1.51 \times 10^4$ s^{-1}) electron exchange on the NMR time scale. In these conditions, signals from the sixteen redox microstates are averaged in five oxidation stages, each including the micro-states with the same number of oxidised haems [18]. Therefore, the substituents of each haem have different chemical shifts in the five stages and since these paramagnetic shifts are proportional to the degree of oxidation of that particular haem group, they can be used to monitor the oxidation of each haem throughout the redox titration [13].

From the analysis of 2D-EXSY NMR spectra of partially oxidised samples, it was possible to follow seven haem methyl resonances (labelled A–G) in different oxidation stages to their final positions in the oxidised protein (Table 1, Figs. 2 and 3). However, the lack of haem methyl assignments in the fully reduced and fully oxidised forms of fcc$_3$ prevents the use of the conventional strategy to assign the order of oxidation of the haem groups [13]. To overcome this difficulty, mutants of the axial ligands of each haem were produced to assist in the specific assignment of the haem methyl signals. However, the only mutated enzyme obtained was that with the axial ligand of haem IV exchanged. All attempts to produce the recombinant proteins with mutations at the other haems (I, II, and III) gave rise to extremely low levels of expression and very unstable proteins that could not be purified. Consequently, a new assignment strategy was applied which combines: (i) NMR information obtained for both native fcc$_3$ and the mutant (fcc$_3$H61A) with haem IV high spin and (ii) paramagnetic chemical shift predictions for each haem methyl substituent of fcc$_3$.

3.1. Cross-assignment of the haem signals to the crystal structure and order of oxidation of the haem groups

In order to make the specific assignment of the haem methyl signals (A–G), the paramagnetic chemical shifts of each haem methyl group (Table 2) were predicted using an empirical
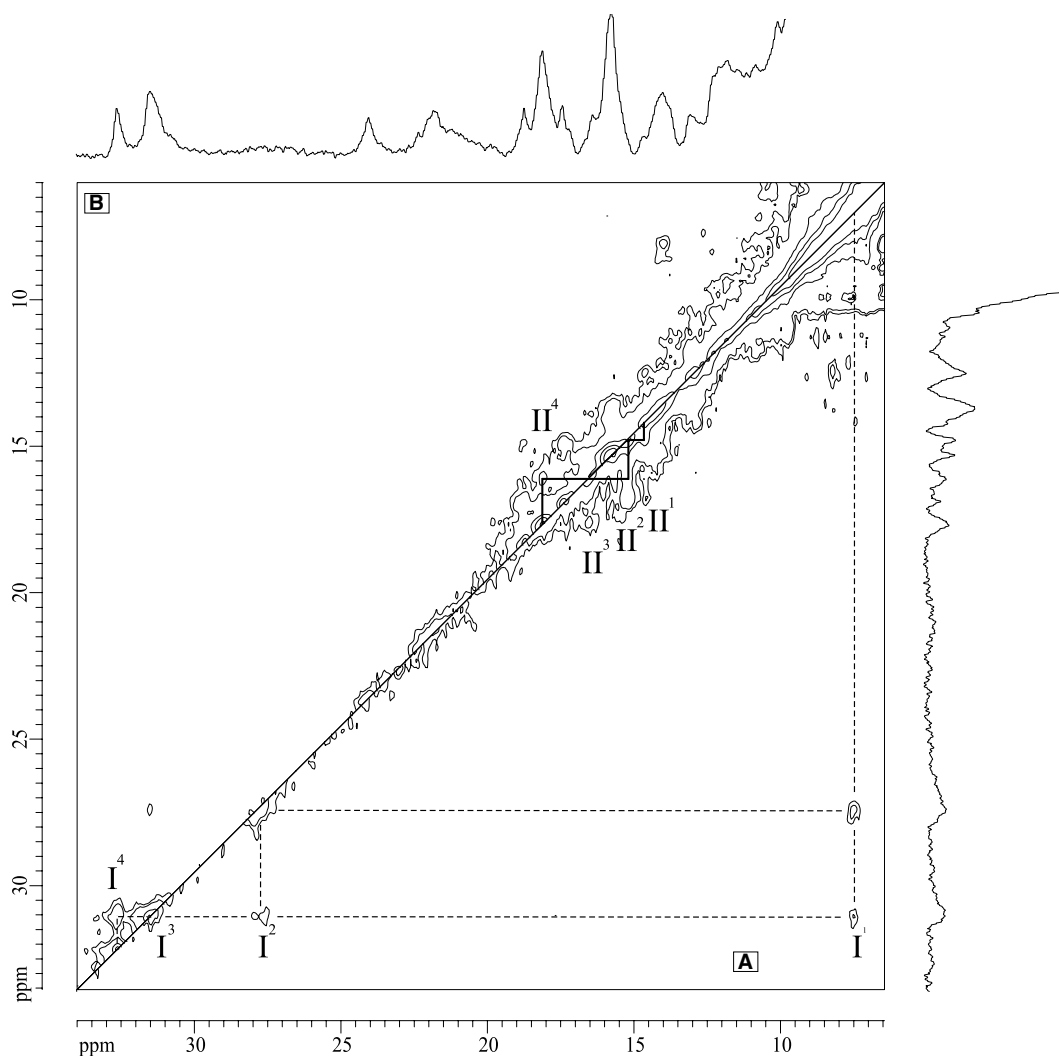
Fig. 2. Region of 2D-EXSY spectra of fcc$_3$ poised at different oxidation levels at pH 8.5 and 298 K. (A) The spectrum shows cross-peaks connecting oxidation stages *1–3*. (B) The spectrum shows cross-peaks connecting oxidation stages *2–4*. The lines connect signals for one methyl group of haem I (dashed lines) and II (solid lines) in different oxidation stages. The Roman and Arabic numbers indicate the haem groups and the oxidation stages, respectively. 1D spectra of the samples are plotted at the edge of the corresponding half-spectra.

Table 1
Redox-dependent ^{1}H haem methyl chemical shifts and haem oxidation fraction of *S. frigidimarina* flavocytochrome c_3, at pH 8.5 and 298 K

Oxidation stage	Chemical shift (ppm)							x_i						
	A	B	C	D	E	F	G	A Haem I	B Haem III	C Haem III	D Haem IV	E Haem III	F Haem II	G Haem IV
0	3.22	(3.48)	(3.48)	(3.48)	(3.48)	3.62	(3.48)	0	0	0	0	0	0	0
1	7.56	n.o.	n.o.	n.o.	n.o.	14.35	n.o.	0.147	n.a.	n.a.	n.a.	n.a.	0.739	n.a.
2	27.60	13.73	10.37	n.o.	n.o.	14.91	n.o.	0.828	0.364	0.337	0.043[a]	n.a.	0.778	0.043[a]
3	31.45	20.06	14.77	12.83	14.50	16.49	8.46	0.959	0.589	0.552	0.499	0.597	0.887	0.473
4	32.66	31.63	23.94	22.20	21.93	18.13	14.00	1	1	1	1	1	1	1

The haem methyls A–G are labelled according to their position in the oxidised form. The haem fractions of oxidation, x_i, in each stage of oxidation are calculated according to the equation $x_i = (\delta_i - \delta_0)/(\delta_4 - \delta_0)$, where δ_i, δ_0, and δ_4 are the observed chemical shifts of the haem methyl in stages *i*, *0*, and *4*, respectively [13]. The chemical shifts indicated in parentheses correspond to the diamagnetic reference for haem methyl protons [30].
n.o., not observed; n.a., not applicable.
[a] Since the sum of the haem oxidation fractions in stage *2* is close to 2, this value was estimated by subtracting the sum of oxidation fraction of haem I (methyl A), haem II (methyl F), and haem III (average of methyls B and C).

equation that uses as input the geometry of the axial ligands in the fcc$_3$ crystal structure. From the analysis of chemical shift predictions (Table 2), the most shifted signal is haem methyl

18^{1}CH$_3^I$ (32.7 ppm), but the experimental data (Table 1) show that two signals, A and B, fall in this region (32.66 and 31.63 ppm, respectively). However, the analysis of the haem methyl
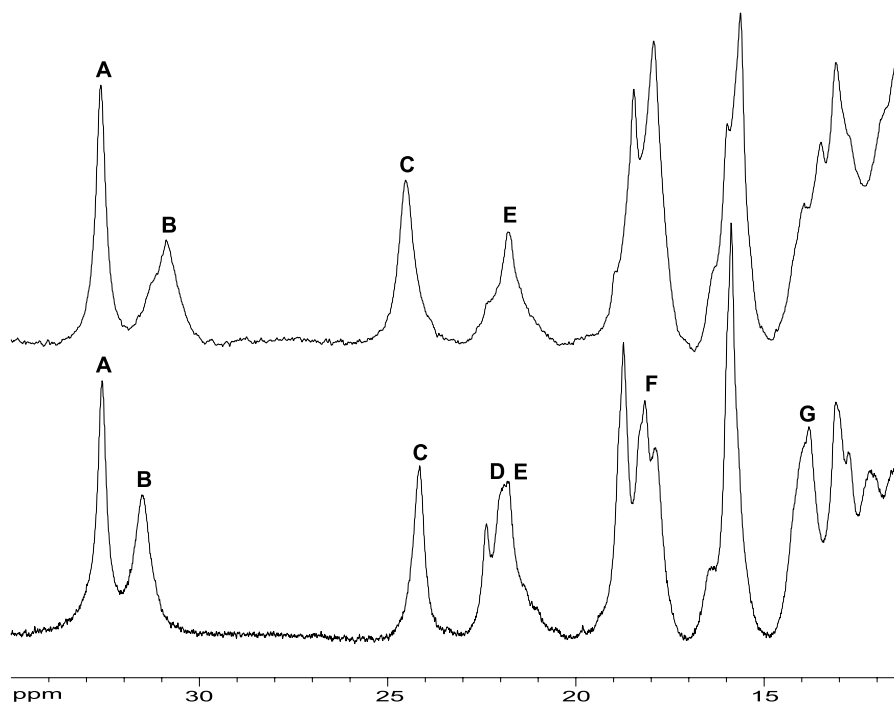
Fig. 3. Low-field region of 300 MHz 1D-^{1}H NMR spectra of the oxidised fcc$_3$ (lower spectrum) and fcc$_3$H61A (upper spectrum) at pH 7.0 and 298 K. The haem methyl signals are labelled alphabetically (A–G).

Table 2
Predicted ^{1}H chemical shifts for each haem methyl in the oxidised *S. frigidimarina* flavocytochrome c_3

Haem methyl	I	II	III	IV
2^1CH_3	10.9	22.0	25.1	20.0
7^1CH_3	15.0	5.2	5.9	7.0
12^1CH_3	12.3	23.4	26.5	21.4
18^1CH_3	32.7	13.7	22.0	13.1

The haem methyls are numbered according to IUPAC-IUB nomenclature for tetrapyrroles [31].

reoxidation patterns (Table 1) shows that the pattern of methyl B is (i) completely different from that of methyl A, which excludes the possibility of these signals belonging to the same haem and (ii) similar to methyl signals C and E, which have chemical shifts of 23.94 and 21.93 ppm, respectively. Since only haem III is expected to have three haem methyl signals above 22.0 ppm (Table 2), this correlates well with signals B, C and E. Therefore, signal A was assigned to $18^1CH_3^I$ and methyls B, C and E to haem III.

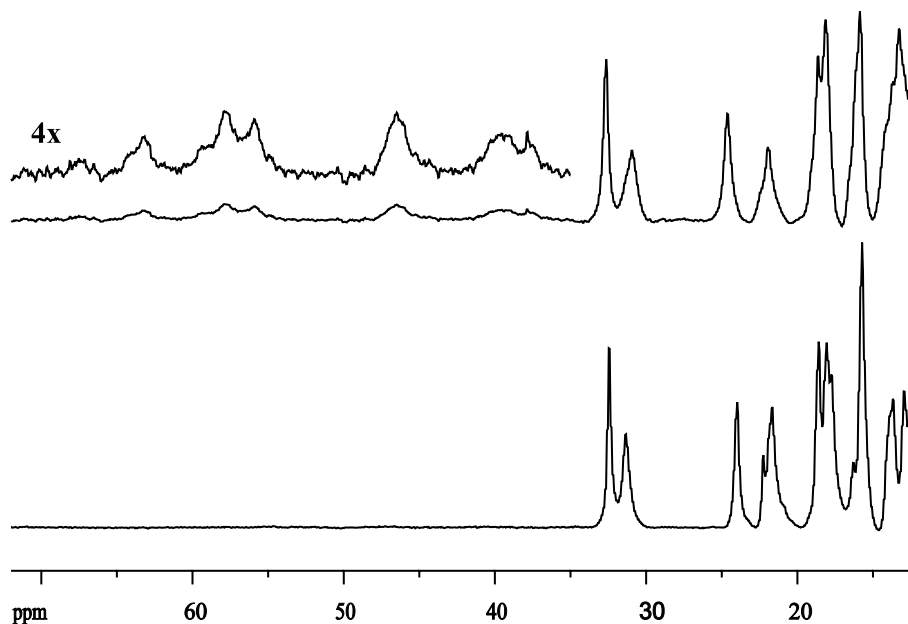Fig. 4. Low-field region of a 300-MHz 1D-^{1}H NMR spectra of the oxidised fcc$_3$ (lower spectrum) and fcc$_3$H61A (upper spectrum) at pH 7.0 and 298 K showing in detail high spin haem methyl signals for fcc$_3$H61A.

The remaining haem methyl signals, which include signals from haems II and IV, appear in more crowded regions of the NMR spectrum (Fig. 3) and, although correlating well with the predictions (Table 2), this is not sufficient to allow unambiguous cross-assignment. In order to distinguish between the signals of haems IV and II, it was necessary to compare the NMR spectra of fcc$_3$ and fcc$_3$H61A. This strategy can be used, since previous studies showed that the crystal structure of fcc$_3$ and fcc$_3$H61A has no significant structural alterations apart from the haem IV axial coordination [11]. In the mutated flavocytochrome, haem IV is a five-coordinated high spin haem and so the NMR signals of the haem substituents are shifted to low field (Fig. 4). Comparison of the 1D-NMR spectra of fcc$_3$ and fcc$_3$H61A (Fig. 3) shows that regions at approximately 22 and 18 ppm are clearly affected, indicating the presence of haem IV signals. From this analysis, haem methyl signals D (22.20 ppm) and F (18.13 ppm) are the best candidates for haem IV. Nonetheless, analysis of the haem oxidation fraction values, in oxidation stages 2 and 3 (Table 1), shows that signals D and F behave quite differently and, therefore, must belong to different haem groups. Thus, in order to elucidate which signal (D or F) belongs to haem IV, 2D-EXSY NMR experiments in partially oxidised fcc$_3$H61A were performed. Comparative analysis of 2D-EXSY NMR spectra of fcc$_3$ and fcc$_3$H61A (data not shown) reveals that the cross-peak corresponding to methyl F, connecting stages 0 and 1, is present in both spectra. Due to the high spin character of haem IV in fcc$_3$H61A, this cross-peak could not belong to haem IV. Thus, signal F must be assigned to haem II and, by exclusion, signal D to haem IV. Finally, signal G was also assigned to haem IV, since it shows a similar oxidation profile to that of signal D.

The assignment strategy applied in this work allowed the unambiguous attribution of the four different oxidation profiles to the respective haem groups in the fcc$_3$ crystal structure (Table 1). The analysis of the haem oxidation fractions of fcc$_3$ (Table 1) reveals that haem II (methyl F) is the more oxidised haem in stage 1, the largest fractional oxidation of haem I (methyl A) is obtained in the step between stages 1 and 2, which is followed by haem III (methyls B, C, E – stage 3) and haem IV (methyls D, G – stage 4).

4. Conclusions

Specific assignments of haem methyl signals to the crystal structure of fcc$_3$ allowed the haem oxidation fractions to be determined, and consequently, the order in which the haems are oxidised. The analysis of the redox behaviour of the haem groups during the redox cycle of fcc$_3$ showed that haems I and II are almost completely oxidised at stage 3 (96% and 89%, respectively), while haems III and IV are only approximately 58% and 49% oxidised, respectively, in this oxidation stage. Since the haem oxidation fractions are similar at pH 8.5 (Table 1) and 7.0 (data not shown), which is close to the pH (7.2) at which this enzyme presents its maximum catalytic efficiency [1], the haem redox behaviour can contribute to our understanding of the functionality of this enzyme. The haem oxidation profiles show that a polarization occurs within the N-terminal haem domain of fcc$_3$ as the oxidation progresses, making two of the haems (haems I and II) much more oxidised when compared with the other two (haems III and IV), haem IV being the most reduced. Since haem IV is simultaneously the closest haem to FAD and presents the highest reduction potential within the tetrahaem domain, thus, during catalysis as an electron is taken by the FAD from haem IV, haem III is energised to promptly re-reduce haem IV, allowing the transfer of two electrons to the active site. In this manner, electrons are always available for transfer from haem IV to FAD, thus maximising the availability of the reduced FAD at the enzyme active site, where fumarate is reduced to succinate.

References

[1] Turner, K.L., Doherty, M.K., Heering, H.A., Armstrong, F.A., Reid, G.A. and Chapman, S.K. (1999) Redox properties of flavocytochrome c_3 from *Shewanella frigidimarina* NCIMB400. Biochemistry 38, 3302–3309.

[2] Gordon, E.H.J., Pealing, S.L., Chapman, S.K., Ward, F.B. and Reid, G.A. (1998) Physiological function and regulation of flavocytochrome c_3, the soluble fumarate reductase from *Shewanella putrefaciens* NCIMB 400. Microbiology 144, 937–945.

[3] Taylor, P., Pealing, S.L., Reid, G.A., Chapman, S.K. and Walkinshaw, M.D. (1999) Structural and mechanistic mapping of a unique fumarate reductase. Nat. Struct. Biol. 6, 1108–1112.

[4] Pealing, S.L., Cheesman, M.R., Reid, G.A., Thomson, A.J., Ward, F.B. and Chapman, S.K. (1995) Spectroscopic and kinetic studies of the tetraheme flavocytochrome c from *Shewanella putrefaciens* NCIMB400. Biochemistry 34, 6153–6158.

[5] Reid, G.A., Gordon, E.H., Hill, A.E., Doherty, M., Turner, K., Holt, R. and Chapman, S.K. (1998) Structure and function of flavocytochrome c_3, the soluble fumarate reductase from *Shewanella* NCIMB400. Biochem. Soc. Trans. 26, 418–421.

[6] Doherty, M.K., Pealing, S.L., Miles, C.S., Moysey, R., Taylor, P., Walkinshaw, M.D., Reid, G.A. and Chapman, S.K. (2000) Identification of the active site acid/base catalyst in a bacterial fumarate reductase: a kinetic and crystallographic study. Biochemistry 39, 10695–10701.

[7] Jones, A.K., Camba, R., Reid, G.A., Chapman, S.K. and Armstrong F.A (2000) Interruption and time-resolution of catalysis by a flavoenzyme using fast scan protein film voltammetry. J. Am. Chem. Soc. 122, 6494–6495.

[8] Jeuken, L.J., Jones, A.K., Chapman, S.K., Cecchini, G. and Armstrong, F.A. (2002) Electron-transfer mechanisms through biological redox chains in multicenter enzymes. J. Am. Chem. Soc. 124, 5702–57013.

[9] Mowat, C.G., Pankhurst, K.L., Miles, C.S., Leys, D., Walkinshaw, M.D., Reid, G.A. and Chapman, S.K. (2002) Engineering water to act as an active site acid catalyst in a soluble fumarate reductase. Biochemistry 41, 11990–11996.

[10] Pankhurst, K.L., Mowat, C.G., Miles, C.S., Leys, D., Walkinshaw, M.D., Reid, G.A. and Chapman, S.K. (2002) Role of His505 in the soluble fumarate reductase from *Shewanella frigidimarina*. Biochemistry 41, 8551–8556.

[11] Rothery, E.L., Mowat, C.G., Miles, C.S., Walkinshaw, M.D., Reid, G.A. and Chapman, S.K. (2003) Histidine 61: an important heme ligand in the soluble fumarate reductase from *Shewanella frigidimarina*. Biochemistry 42, 13160–13169.

[12] Rothery, E.L., Mowat, C.G., Miles, C.S., Mott, S., Walkinshaw, M.D., Reid, G.A. and Chapman, S.K. (2004) Probing domain mobility in a flavocytochrome. Biochemistry 43, 4983–4989.

[13] Salgueiro, C.A., Turner, D.L., Santos, H., LeGall, J. and Xavier, A.V. (1992) Assignment of the redox potentials to the four haems in *Desulfovibrio vulgaris* cytochrome c_3 by 2D NMR. FEBS Lett. 314, 155–158.

[14] Louro, R.O., Pacheco, I., Turner, D.L., LeGall, J. and Xavier, A.V. (1996) Structural and functional characterization of

cytochrome c_3 from *D. desulfuricans* ATCC 27774 by ^{1}H NMR. FEBS Lett. 390, 59–62.

[15] Pessanha, M., Brennan, L., Xavier, A.V., Cuthbertson, P.M., Reid, G.A., Chapman, S.K., Turner, D.L. and Salgueiro, C.A. (2001) NMR structure of the haem core of a novel tetrahaem cytochrome isolated from *Shewanella frigidimarina*: identification of the haem-specific axial ligands and order of oxidation. FEBS Lett. 489, 8–13.

[16] Pessanha, M., Londer, Y.Y., Long., W.C., Erickson, J., Pokkuluri, P.R., Schiffer, M. and Salgueiro, C.A. (2004) Redox characterization of *Geobacter sulfurreducens* cytochrome c_7: physiological relevance of the conserved residue F15 probed by site-specific mutagenesis. Biochemistry 43, 9909–9917.

[17] Santos, H., Turner, D.L., Xavier, A.V. and LeGall, J. (1984) Two-dimensional NMR studies of electron transfer in cytochrome c_3. J. Magn. Reson. 59, 177–180.

[18] Santos, H., Moura, J.J.G., Moura, I., LeGall, J. and Xavier, A.V. (1984) NMR studies of electron transfer mechanisms in a protein with interacting redox centres: *Desulfovibrio gigas* cytochrome c_3. Eur. J. Biochem. 141, 283–296.

[19] Park, J.S., Ohmura, T., Kano, K., Sagara, T., Niki, K., Kyogoku, Y. and Akutsu, H. (1996) Regulation of the redox order of four hemes by pH in cytochrome c_3 from *D. vulgaris* Miyazaki F. Biochim. Biophys. Acta 1293, 45–54.

[20] Turner, D.L., Salgueiro, C.A., Catarino, T., LeGall, J. and Xavier, A.V. (1996) NMR studies of cooperativity in the tetrahaem cytochrome c_3 from *Desulfovibrio vulgaris*. Eur. J. Biochem. 241, 723–731.

[21] Louro, R.O., Catarino, T., Turner, D.L., Piçarra-Pereira, M.A., Pacheco, I., LeGall, J. and Xavier, A.V. (1998) Functional and mechanistic studies of cytochrome c_3 from *Desulfovibrio gigas*: thermodynamics of a proton thruster. Biochemistry 37, 15808–15815.

[22] Louro, R.O., Catarino, T., LeGall, J., Turner, D.L. and Xavier, A.V. (2001) Cooperativity between electrons and protons in a monomeric cytochrome c_3: the importance of mechano-chemical coupling for energy transduction. ChemBioChem 2, 831–837.

[23] Correia, I.J., Paquete, C.M., Louro, R.O., Catarino, T., Turner, D.L. and Xavier, A.V. (2002) Thermodynamic and kinetic characterization of trihaem cytochrome c_3 from *Desulfuromonas acetoxidans*. Eur. J. Biochem. 269, 5722–5730.

[24] Harada, E., Kumagai, J., Ozawa, K., Imabayashi, S., Tsapin, A.S., Nealson, K.H., Meyer, T.E., Cusanovich, M.A. and Akutsu, H. (2002) A directional electron transfer regulator based on heme-chain architecture in the small tetraheme cytochrome *c* from *Shewanella oneidensis*. FEBS Lett. 532, 333–337.

[25] Pereira, P.M., Pacheco, I., Turner, D.L. and Louro, R.O. (2002) Structure–function relationship in type II cytochrome c_3 from *Desulfovibrio africanus*: a novel function in a familiar heme core. J. Biol. Inorg. Chem. 7, 815–822.

[26] Reis, C., Louro, R.O., Pacheco, I., Catarino, T., Turner, D.L. and Xavier, A.V. (2002) Redox-Bohr effect in the nine haem cytochrome from *Desulfovibrio desulfuricans* 27774. Inorg. Chim. Acta 339, 248–252.

[27] Pessanha, M., Louro, R.O., Correia, I.J., Rothery, E.L., Pankhurst, K.L., Reid, G.A., Chapman, S.K., Turner, D.L. and Salgueiro, C.A. (2003) Thermodynamic characterization of a tetrahaem cytochrome isolated from a facultative aerobic bacterium, *Shewanella frigidimarina*: a putative redox model for flavocytochrome c_3. Biochem. J. 370, 489–495.

[28] Kyritsis, P., Huber, J.G., Quinkal, I., Gaillard, J. and Moulis, J. (1997) Intramolecular electron transfer between [4Fe–4S] clusters studied by proton magnetic resonance spectroscopy. Biochemistry 36, 7839–7846.

[29] Turner, D.L. (2000) Obtaining ligand geometries from paramagnetic shifts in low-spin haem proteins. J. Biol. Inorg. Chem. 5, 328–332.

[30] Piçarra-Pereira, M.A., Turner, D.L., LeGall, J. and Xavier, A.V. (1993) Structural studies on *Desulfovibrio gigas* cytochrome c_3 by two-dimensional [1]H-nuclear-magnetic-resonance spectroscopy. Biochem. J. 294, 909–915.

[31] Moss, G.P. (1988) Nomenclature of tetrapyrroles. Recommendations 1986 IUPAC-IUB Joint Commission on Biochemical Nomenclature (JCBN). Eur. J. Biochem. 178, 277–328.